

and

$$X_i(s'; \tau, \xi) = \xi - \int_{s(\tau, \xi)}^{s'} f_i^1\{t(s), X_i(s; \tau, \xi)\} ds \quad (A5)$$

$$i = 1, 2, \dots, n.$$

The initial data  $v_i[t(0), X_i(0; \tau, \xi)]$  ( $i = 1, 2, \dots, n$ ) of (A4) are the values of  $v_i(i = 1, 2, \dots, n)$  on the initial curve at the points  $[t(0), X_i(0; \tau, \xi)]$  ( $i = 1, 2, \dots, n$ ) of  $I \times E$  located by tracing back  $X_i(s'; \tau, \xi)$  from  $(\tau, \xi)$  according to the rule (A5). The values of  $v_i(i = 1, 2, \dots, n)$  (or the value of  $v$  at any point of the initial curve) are given by the initial and boundary conditions in (4) and (5).

The characteristics for the vector  $\mu (= \partial v / \partial x)$  of the system (1) can be derived from the general system of the first-order equations:

$$F(t, x, v, \lambda, \mu, u) = 0 \quad (A6)$$

where  $F = (F_1, F_2, \dots, F_n)'$  and  $\lambda = (\lambda_1, \lambda_2, \dots, \lambda_n)' = \left( \frac{\partial v_1}{\partial t}, \frac{\partial v_2}{\partial t}, \dots, \frac{\partial v_n}{\partial t} \right)'$ . Partial differentiation of (A6) with respect to  $x$  yields

$$F_x + (\nabla_v F) \mu + (\nabla_\lambda F) \frac{\partial \lambda}{\partial x} + (\nabla_\mu F) \frac{\partial \mu}{\partial x} = 0 \quad (A7)$$

In view of the identity  $\partial \lambda / \partial x = \partial \mu / \partial t$ , it follows that

$$(\nabla_\lambda F) \frac{\partial \mu}{\partial t} + (\nabla_\mu F) \frac{\partial \mu}{\partial x} = -F_x - (\nabla_v F) \mu \quad (A8)$$

For the system (1),  $\nabla_\lambda F = I$ , and  $\nabla_\mu F$  is a diagonal matrix, so that the system (A8) is in canonical form. Thus the characteristic equations for  $\mu$  are

$$\frac{dx}{ds} = \nabla_\mu F$$

$$\frac{d\mu}{ds} = -F_x - (\nabla_v F) \mu \quad (A9)$$

In connection with the system (1), the first equation in (A10) is identical to (A2) for  $\nabla_\mu F = -f^1$ . The second equation becomes explicitly

$$\frac{d\mu}{ds} = \phi(t(s), x, v, \mu, u) \quad (A11)$$

where  $\phi = (\phi_1, \phi_2, \dots, \phi_n)' = f_x + (\nabla_v f) \mu$ .

On the line  $t = t_0$  the initial values  $\mu$  are, from Equation (4),

$$\mu(t_0, x) = \frac{d\Phi(x)}{dx} \quad (A12)$$

On the remaining segment of the initial curve (the line  $x = x_0$ ) the values of the initial data of  $\mu$  can be shown, from Equation (5), to be given by

$$\mu_i[t(o), x_0] = \frac{\left[ f_i^0\{t(o), x_0, \Psi_i[t(o)], u[t(o), x_0]\} - \frac{d\Psi_i(t)}{dt} \right] \left| \frac{dt}{ds} \right|_{s=0}}{[-f_i^1\{t(o), x_0, u[t(o), x_0]\}]} \\ = \Pi_i \left\{ t(o), x_0, \Psi_i[t(o)], \frac{d\Psi_i[t(o)]}{dt}, \frac{dt(o)}{ds}, u[t(o), x_0] \right\} \quad (A13)$$

$$i = 1, 2, \dots, n$$

The expressions (A13) are the initial data  $\mu_i[t(o), X_i(o; \tau, \xi)]$  of (A11) along the segment (the line  $x = x_0$ ). An interesting observation is that the initial data are functions of  $u$ . Here  $f_i^1\{t(o), x_0, u[t(o), x_0]\} \neq 0$ . If  $f_i^1 = 0$ , the initial curve ( $x = x_0$ ) is a characteristic. This situation is excluded from the development.

## Part II. Jacketed Configuration with Step Feed Disturbance

The optimal unsteady control of a jacketed tubular reactor with and without heat generation due to chemical reaction in response to a step disturbance in the feed stream concentration is computed. More rigorous control action was found to be necessary for the case with heat generation than without heat generation. Convergence of the method was also investigated with fixed and free final time.

### STATEMENT OF PROBLEM

The optimal control of a jacketed tubular reactor is considered, in which the first-order consecutive reactions  $A \xrightarrow{k_1} B \xrightarrow{k_2} C$  take place, both with and without heat generation. The shell-side fluid temperature,  $u$ , is the control, where  $u = u(t)$  only. It is desired to obtain the optimal control,  $\hat{u}(t)$ , with a known step disturbance in the inlet concentration, such that the cumulative yield of the desired product  $B$  at the exit  $x = L$  during a specified time interval  $[0, t_f]$  is maximized. The system of partial differential equations for the process is

$$\begin{aligned} \frac{\partial v_1}{\partial t} &= -k_1 v_1 - \nu \frac{\partial v_1}{\partial x} \\ \frac{\partial v_2}{\partial t} &= k_1 v_1 - k_2 v_2 - \nu \frac{\partial v_2}{\partial x} \\ \frac{\partial v_3}{\partial t} &= b_1 k_1 v_1 + b_2 k_2 v_2 + \frac{1}{\alpha} [u(t) - v_3] - \nu \frac{\partial v_3}{\partial x} \end{aligned} \quad (1)$$

subject to the initial and boundary conditions

$$v_i(0, x) = \Phi_i(x), \quad v_i(t, 0) = \Psi_i(t) \quad i = 1, 2, 3 \quad (2)$$

where  $k_i = k_{i0} \exp(-E_i/RT)$  ( $i = 1, 2$ ), and  $\Phi_i(x)$  and

$\Psi_i(t)$  are prescribed functions of  $x$  and of  $t$ , respectively. This problem has been discussed earlier (1), where now the functional to be minimized is

$$- \int_0^{t_f} v_2(t, L) dt \quad \text{or} \quad J = \int_0^{t_f} \int_0^L \left( -\frac{\partial v_2}{\partial x} \right) dx dt \quad (3)$$

The numerical values for the physical constants involved are taken from the work of Bilous and Amundson (2):  $k_{10} = 0.535 \times 10^{11} \text{ min.}^{-1}$ ,  $k_{20} = 0.461 \times 10^{18} \text{ min.}^{-1}$ ,  $E_1 = 18 \text{ kcal./mole}$ ,  $E_2 = 30 \text{ kcal./mole}$ , and  $R = 2.0$ . In addition, let  $\alpha = 3.0$ ,  $L = 1$  unit of length and  $\nu = 0.1$  unit of length/min., thus fixing the residence time at 10 min.

### Negligible Heat Generation

Suppose that it has been previously determined, by a gradient method, that the optimal steady state, with negligible heat of reaction and for inlet concentrations  $v_1(0)$  and  $v_2(0)$  of 0.95 and 0.5 g. mole/liter, is obtained by choosing  $v_3(0) = 349.3^\circ \text{K.}$  and  $u = 335.5^\circ \text{K.}$  up to the time  $t = 0^-$ . At  $t = 0^+$ , the inlet concentrations suddenly change to  $v_1(0) = 0.65$  and  $v_2(0) = 0.35$  g. mole/liter, and the feed temperature to  $v_3(0) = 300^\circ \text{K.}$  It is required to find the control  $u(t)$  such that the cumulative yield  $v_2(1)$  is maximized during the time interval  $[0, t_f]$ . The original and new optimal steady states are plotted in Fig-

ures 1 and 2, and the results summarized in Table 1.

TABLE 1. STEADY STATES

| $v_1(0)$ | $v_2(0)$ | Optimal<br>$v_3(0)$ , °K. | Optimal<br>$u$ , °K. | Optimal<br>Yield<br>$v_2$ at $x = 1$ |
|----------|----------|---------------------------|----------------------|--------------------------------------|
| 0.95     | 0.05     | 349.3                     | 335.5                | 0.6797                               |
| 0.65     | 0.35     | 300.0                     | 344.8                | 0.6779                               |

The Hamiltonian function is given by (1):

$$H \equiv \frac{\partial v_2}{\partial x} + p_1 \left( -k_1 v_1 - \nu \frac{\partial v_1}{\partial x} \right) + p_2 \left( k_1 v_1 - k_2 v_2 - \nu \frac{\partial v_2}{\partial x} \right) + p_3 \left[ b_1 k_1 v_1 + b_2 k_2 v_2 + \frac{1}{\alpha} (u(t) - v_3) - \nu \frac{\partial v_3}{\partial x} \right] \quad (4)$$

The auxiliary system is then

$$\begin{aligned} \frac{\partial p_1}{\partial t} &= k_1 p_1 - k_1 p_2 - b_1 k_1 p_3 - \nu \frac{\partial p_1}{\partial x} \\ \frac{\partial p_2}{\partial t} &= k_2 p_2 - b_2 k_2 p_3 - \nu \frac{\partial p_2}{\partial x} \\ \frac{\partial p_3}{\partial t} &= \frac{E_1}{Rv_3^2} k_1 v_1 p_1 - \frac{1}{Rv_3^2} (E_1 k_1 v_1 - E_2 k_2 v_2) p_2 \\ &\quad - \frac{1}{Rv_3^2} (b_1 E_1 k_1 v_1 + b_2 E_2 k_2 v_2) p_3 \\ &\quad + \frac{p_3}{\alpha} - \nu \frac{\partial p_3}{\partial x} \end{aligned} \quad (5)$$

The systems of characteristic equations are

$$\frac{dv_1}{ds} = -k_1 v_1$$

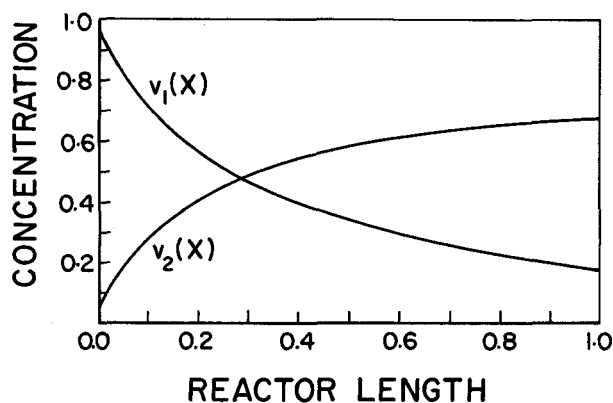
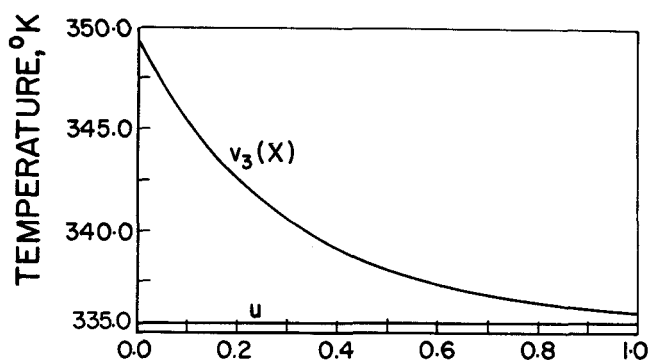


Fig. 1. Optimal steady state for  $v_1(0) = 0.95$  and  $v_2(0) = 0.05$  g.mole/liter,  $b_1 = 0$ ,  $b_2 = 0$ ,  $\alpha = 3.0$ .

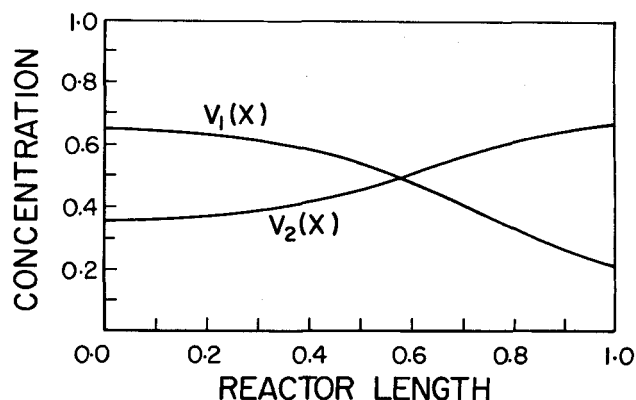
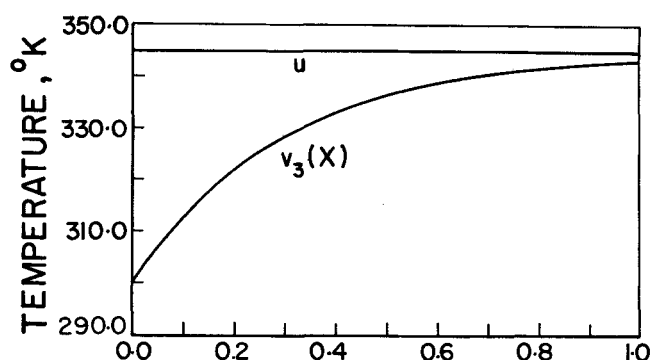


Fig. 2. Optimal steady state for  $v_1(0) = 0.65$ ,  $v_2(0) = 0.35$  g.mole/liter, and  $v_3(0) = 300^\circ\text{K}$ ,  $b_1 = 0$ ,  $b_2 = 0$ ,  $\alpha = 3.0$ .

$$\frac{dv_2}{ds} = k_1 v_1 - k_2 v_2$$

$$\frac{dv_3}{ds} = b_1 k_1 v_1 + b_2 k_2 v_2 + \frac{1}{\alpha} [u(t) - v_3] \quad (6)$$

and

$$\frac{dp_1}{ds} = k_1 p_1 - k_1 p_2 - b_1 k_1 p_3$$

$$\frac{dp_2}{ds} = k_2 p_2 - b_2 k_2 p_3$$

$$\begin{aligned} \frac{dp_3}{ds} &= \frac{E_1}{Rv_3^2} k_1 v_1 p_1 - \frac{1}{Rv_3^2} (E_1 k_1 v_1 - E_2 k_2 v_2) p_2 \\ &\quad - \frac{1}{Rv_3^2} (b_1 E_1 k_1 v_1 + b_2 E_2 k_2 v_2) p_3 + \frac{p_3}{\alpha} \end{aligned} \quad (7)$$

with the initial data in Equation (2) and  $p_i(\sigma, 1) = \delta_{i2}/\nu$  ( $i = 1, 2, 3$ ). The relationship between  $s$  and  $t$  is given by  $s(\sigma, L) - s = \sigma - t$ . For this case  $b_1 = b_2 = 0$ . A computational algorithm is (1)

$$u^{(i+1)} = u^{(i)} + \epsilon^{(i)} \int_0^1 \left( \frac{p_3}{\alpha} \right) dx \quad (8)$$

The reactor length  $[0, 1]$  was divided into 20 sections, giving a mesh size  $\Delta x = 0.05$ . Since  $\nu = 0.1$ , this fixes  $\Delta t = 0.5$  min. An initial guess was made of  $u(t)$  for  $t \in [0, t_f]$ . The values of  $u(t)$  were assigned at the time-mesh points and the values between mesh points interpolated. A fourth-order Runge-Kutta method was used for the integration along the characteristic line with a step size  $\Delta s = 0.01$ . In the integration of Equation (6), the values of  $v_1$ ,  $v_2$ , and  $v_3$  were stored for the backward integration of Equation (7). At the end of each integration, only the values  $p_3/\alpha$  were stored at the grid points for the next iteration. When the numerical values of  $p_3/\alpha$

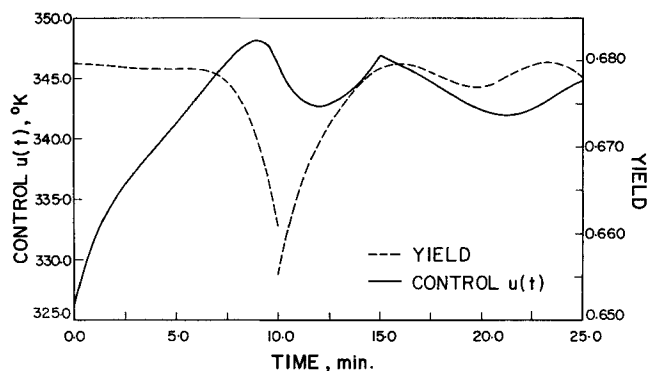


Fig. 3. Optimal control  $u(t)$  and optimal yield  $v_2(t,1)$  for  $t_f = 25$  min.,  $b_1 = 0$ ,  $b_2 = 0$ .

were available over the entire grid points, the integral  $\int_0^1 p_3/\alpha dx$  was evaluated by Simpson's one-third rule and three-eighths rule. The discontinuity due to the step disturbance carries itself along the characteristic line. Therefore, along this line the integration of (6) and (7) must be carried out twice: once with initial conditions  $\Phi_i(0)$  ( $i = 1, 2, 3$ ), and once with the boundary conditions  $\Psi_i(0)$  ( $i = 1, 2, 3$ ). This, in turn, creates odd and even panels in the integration of  $\int_0^1 p_3/\alpha dx$  which demands the use of the two rules. At each time-mesh point an improved control was obtained by Equation (8). The storage locations used for the integration of the equations in (6) and (7) along one characteristic could be used again for the same purpose along another characteristic.

The optimal control  $u(t)$  and the corresponding optimal yield  $v_2(t,1)$ , obtained for  $t_f = 25, 40$ , and  $55$  min., are plotted in Figures 3, 4, and 5. At  $t = 0^+$ ,  $u(t)$  drops below the steady state value, and then gradually increases to a peak. It then settles down with a damped oscillation to the new steady state optimal control, but exhibits a second sharp hump one residence time ahead of the time  $t_f$ . The physical explanation is that the control within one residence time from  $t_f$  does not have to be optimal for the portion of the reactant fluid still in the reactor at the final time  $t_f$ . The effect of the hump is shown at the tail portion of the yield curves. The optimal yield curves in these figures are all discontinuous at  $t = 10$  min., owing to propagation of the discontinuity  $\Phi(0) \neq \Psi(0)$  along the characteristic line.

If the portions of the optimal control curves less than one residence time from  $t_f$  are excluded, and the remaining portions plotted on the same graph, the result is Figure 6. The shapes of optimal controls for  $t_f = 25, 40$ , and  $55$  min. coincide. Hence the structure of the optimal control  $u(t)$  appears to be independent of  $t_f$  for  $t < t_f - t_r$ , where  $t_r$  is the residence time.

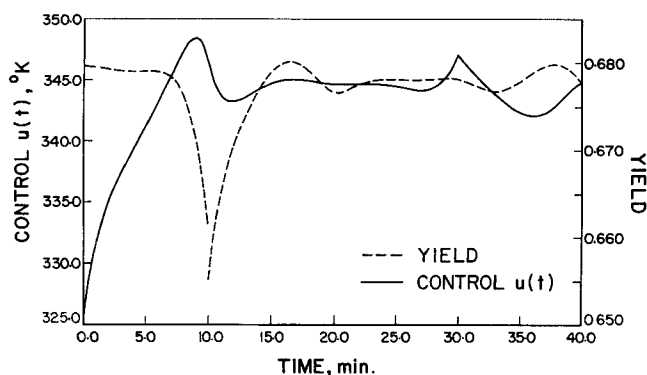


Fig. 4. Optimal control  $u(t)$  and optimal yield  $v_2(t,1)$  for  $t_f = 40$  min.,  $b_1 = 0$ ,  $b_2 = 0$ .

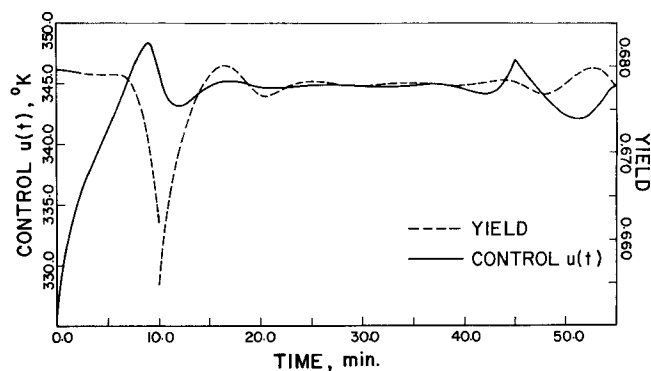


Fig. 5. Optimal control  $u(t)$  and optimal yield  $v_2(t,1)$  for  $t_f = 55$  min.,  $b_1 = 0$ ,  $b_2 = 0$ .

As shown in Table 2, the optimum is quite flat:

TABLE 2. CUMULATIVE YIELD  $\int_0^{t_f} v_2(t,1)dt$  TO STEP

DISTURBANCE

$b_1 = 0$ ,  $b_2 = 0$ , and  $\alpha = 3.0$

| $[0, t_f]$<br>min. | No. of<br>Iterations | Optimal<br>Cumulative<br>Yield | Cumulative<br>Yield with<br>No Control<br>Action | Cumulative<br>Yield with<br>Instantaneous<br>Application<br>of New<br>Steady State<br>Optimal<br>Control |
|--------------------|----------------------|--------------------------------|--|--|
| 25                 | 16                   | 16.914                         | 16.067   | 16.697   |
| 40                 | 21                   | 27.083                         | 25.337   | 26.865   |
| 55                 | 18                   | 37.251                         | 34.607   | 37.034   |

The same problem was now investigated with heat generation ( $b_1 = 100$  and  $b_2 = -50$ ). The original and the new steady state profiles are plotted in Figures 7 and 8, respectively. The profiles in Figure 7 serve as the initial conditions in (2). The optimal temperature profile for the new steady state is a monotonically increasing profile with only the rear half of the reactor now being cooled, with results shown in Table 3.

The optimal control  $u(t)$  for  $t_f = 40$  min. is plotted in Figure 9. The sharp hump still exists, as before, at one

TABLE 3. STEADY STATES

| $v_1(0)$ | $v_2(0)$ | Optimal<br>$v_3(0), ^\circ K.$ | Optimal<br>$u, ^\circ K.$ | Optimal<br>Yield<br>$v_2$ at $x = 1$ |
|----------|----------|--------------------------------|---------------------------|--------------------------------------|
| 0.95     | 0.05     | 331.4                          | 316.4                     | 0.6628                               |
| 0.65     | 0.35     | 300.0                          | 331.7                     | 0.6658                               |

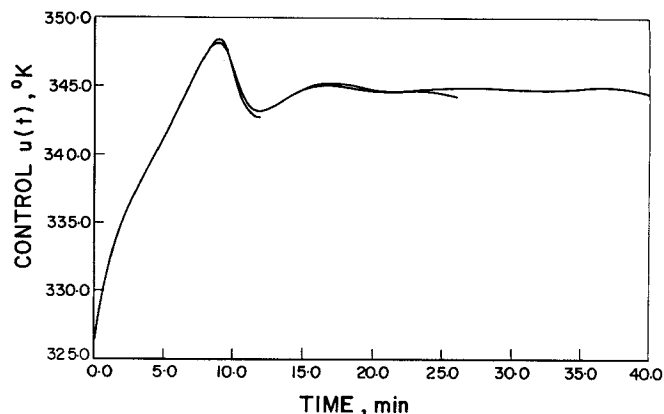


Fig. 6. Optimal controls for  $t_f = 25, 40$ , and  $55$  min.,  $t < t_f - 10$ ,  $b_1 = 0$ ,  $b_2 = 0$ .

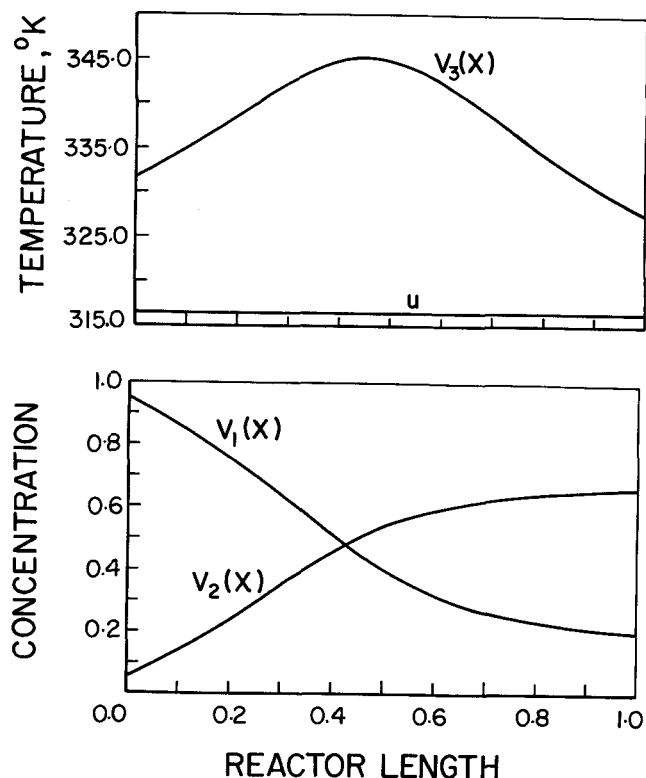


Fig. 7. Optimal steady state for  $v_1(0) = 0.95$  and  $v_2(0) = 0.05$  g.mole/liter,  $b_1 = 100$ ,  $b_2 = -50$ ,  $\alpha = 3.0$ .

residence time ahead of the final time  $t_f$ . The amplitude of the damped oscillatory control is larger than that of the reactor without heat generation. The corresponding optimal yield curves are also plotted as dashed lines. The yield curves are also more oscillatory than before, and the discontinuity due to  $\Phi(0) \neq \Psi(0)$  is now almost unnoticeable. A plot of optimal controls for  $t_f = 25, 40$ , and  $55$  min. excluding the final humps, is shown in Figure 10. The patterns are almost the same, although the oscillation

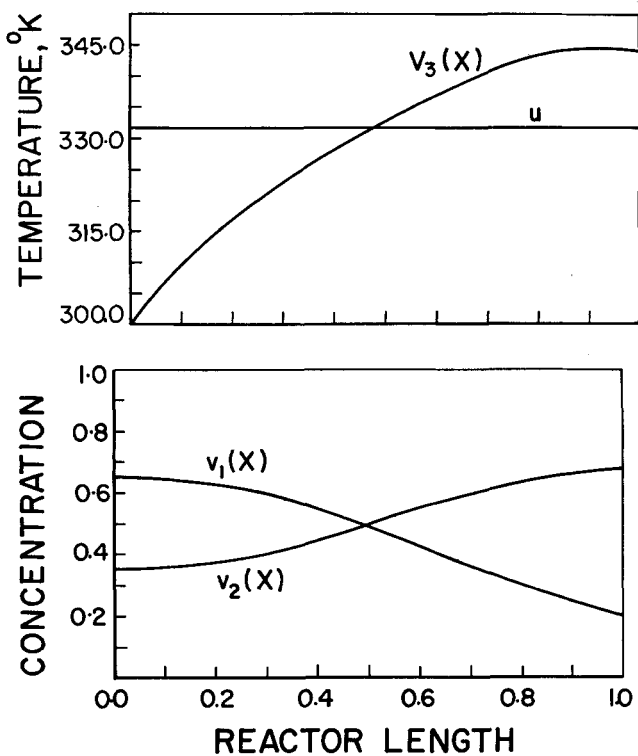


Fig. 8. Optimal steady state for  $v_1(0) = 0.65$ ,  $v_2(0) = 0.35$  g.mole/liter, and  $v_3(0) = 300^\circ\text{K}$ ,  $b_1 = 100$ ,  $b_2 = -50$ ,  $\alpha = 3.0$ .

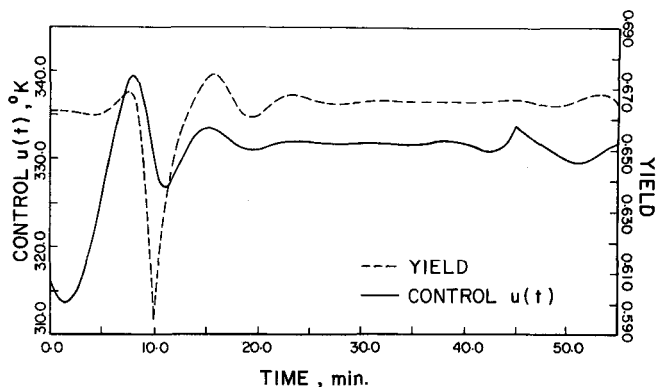


Fig. 9. Optimal control  $u(t)$  and optimal yield  $v_2(t, 1)$  for  $t_f = 40$  min.,  $b_1 = 100$ ,  $b_2 = -50$ .

amplitude is larger for smaller  $t_f$ , with the valleys and the peaks occurring at the same positions in time. One concludes that the optimal control  $u(t)$  as  $t_f \rightarrow \infty$  must exhibit the same oscillation with somewhat a smaller amplitude.

If no control action is taken against the step disturbance, the yield is considerably smaller, as shown in Figure 11. The instantaneous application of the optimal control for the new steady state would also give a smaller yield than the application of the optimal control during the first interval of the residence time. The results are summarized in Table 4.

TABLE 4. CUMULATIVE YIELD  $\int_0^{t_f} v_2(t, 1) dt$  TO STEP DISTURBANCE

$b_1 = 100$ ,  $b_2 = -50$ , and  $\alpha = 3.0$

| $[0, t_f]$<br>min. | No. of<br>Iterations | Optimal<br>Cumulative<br>Yield | Cumulative<br>Yield with<br>No Control<br>Action | Cumulative<br>Yield with<br>Instantaneous<br>Application<br>of New<br>Steady State<br>Optimal<br>Control |
|--------------------|----------------------|--------------------------------|--|--|
| 25                 | 28                   | 16.518                         | 13.664   | 15.497   |
| 40                 | 25                   | 26.499                         | 20.700   | 25.485   |
| 55                 | 23                   | 36.480                         | 27.736   | 35.471   |

#### CONVERGENCE OF ITERATION

One can check whether the optimal control has been reached by repeating the computation with a different starting function for  $u(t)$ . This has been done for the previous problems, and in each case, two separate computations converged to the same optimal control  $u(t)$ .

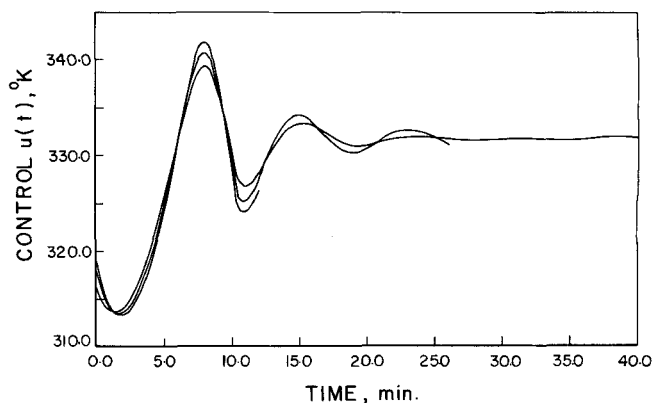


Fig. 10. Optimal controls for  $t_f = 25, 40$ , and  $55$  min.,  $t < t_f - 10$ ,  $b_1 = 100$ ,  $b_2 = -50$ .

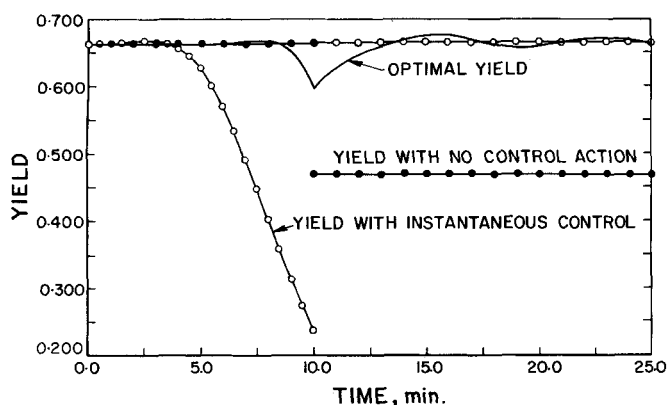


Fig. 11. Yield with no control and with instantaneous new steady state control,  $t_f = 25$  min.,  $b_1 = 100$ ,  $b_2 = -50$ .

Because of the more strongly oscillatory nature of the optimal control, more iterations were necessary for the case with heat generation. In every case, rapid convergence was observed by the fifth to tenth iteration.

It may be noted that the final time condition on the adjoint variables requires that  $p_3(x, t_f) = 0$ . Hence, any choice of  $u(t_f)$  cannot be improved by the algorithm (8). The neighborhood points are also affected in the numerical computation. In the previous iterative computations, the control at this point was fixed at the optimal  $u$  for the new steady state from the physical reasoning that the optimal control must eventually converge to the optimal control of the final steady state. For small  $t_f$ , the effect of using different controls at the singular point on the entire optimal control profile deserves investigation. Five different values of  $u$  were used at  $t_f = 20$  min. for the case with heat generation; 347.1, 339.4, 324.1, 316.4, and the optimal  $u$ , 331.7°K. The optimal control profiles and the corresponding yields are plotted in Figure 12. The cumulative yields were 13.1780, 13.1797, 13.1799, 13.1776, and 13.1803 g. moles for a 1 liter/min. flow rate, respectively, justifying the choice of  $u(t_f)$  to be that for the new steady state.

If, in addition, the condition that the process should reach the new steady state at time  $t = t_f$  be imposed, the control  $u(t)$  must be set to the optimal  $u$  for the new steady state one residence time ahead of time  $t_f$ . For the remaining portion of the time interval, the control is such that the cumulative yield of  $v_2$  over the entire interval be maximum. For the numerical computation,  $t_f = 30$  min. was taken. The optimal control and yield obtained from the iterative computations are plotted in Figure 13 for the case with  $b_1 = b_2 = 0$ . The optimal control of the previous problem with  $t_f = 45$  min. is also plotted. Up to  $t = 20$  min., the two controls coincide well. From these results it can be concluded that the structure of the optimal control with fixed transfer time is basically not different from the one without specified transfer time.

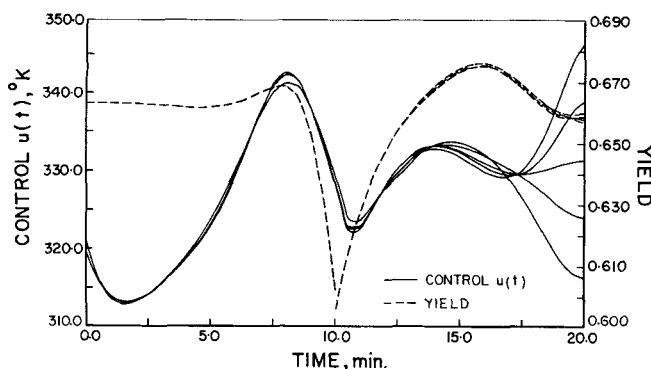


Fig. 12. Effect of  $u$  at  $t = t_f$ ;  $b_1 = 100$ ,  $b_2 = -50$ .

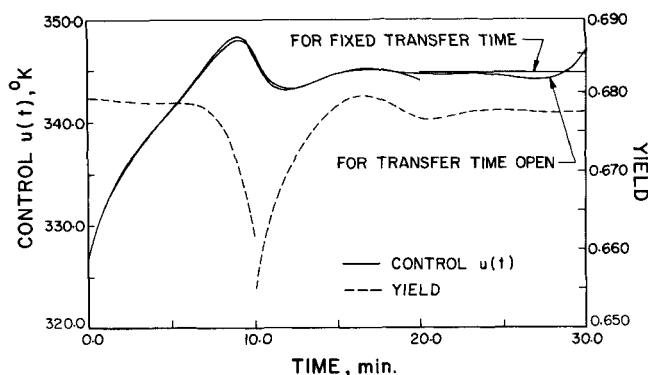


Fig. 13. Optimal control and optimal yield with fixed transfer time,  $t_f = 30$  min.,  $b_1 = 0$ ,  $b_2 = 0$ .

## ACKNOWLEDGMENT

This work was supported by the National Science Foundation (N.S.F. Grant GK-1126) and by I.P.A.C. System Laboratory, Northwestern University (Defense Department Contract N00014-66-CO20A03). A generous grant of computer time by Northwestern University Computing Center is also acknowledged.

## NOTATION

|                          |  |
|--------------------------|--|
| $b_1, b_2$               | $= (-\Delta H_1)/C_p \cdot \rho, (-\Delta H_2)/C_p \cdot \rho$ |
| $C_p$                    | $=$ specific heat  |
| $E_1, E_2$               | $=$ activation energies  |
| $\mathcal{G}$            | $=$ integrand of functional $J$                                |
| $H$                      | $=$ function defined by $-\mathcal{G} + \langle p, f \rangle$  |
| $\Delta H_1, \Delta H_2$ | $=$ heat of reactions  |
| $J$                      | $=$ functional   |
| $k_1, k_2$               | $=$ rate constants   |
| $k_{10}, k_{20}$         | $=$ pre-exponential factors                                    |
| $L$                      | $=$ length   |
| $p_1, p_2, p_3$          | $=$ auxiliary variables  |
| $R$                      | $=$ gas constant   |
| $r$                      | $=$ radius of tube   |
| $s$                      | $=$ parameter along characteristic curve                       |
| $T$                      | $=$ temperature, $v_3$   |
| $t$                      | $=$ time variable  |
| $t_f$                    | $=$ final time   |
| $U$                      | $=$ overall heat transfer coefficient                          |
| $u$                      | $=$ control  |
| $v_1, v_2, v_3$          | $=$ state variables  |
| $x$                      | $=$ distance variable  |

## Greek Letters

|               |  |
|---------------|--|
| $\alpha$      | $=$ heat exchange parameter, $\tau C_p \rho / 2U$            |
| $\Delta$      | $=$ increment  |
| $\delta_{ij}$ | $=$ Kronecker delta  |
| $\epsilon$    | $=$ iteration step size                                      |
| $\nu$         | $=$ velocity of fluid  |
| $\rho$        | $=$ density  |
| $\Phi$        | $=$ initial state vector, $(\Phi_1, \Phi_2, \dots, \Phi_n)$  |
| $\Psi$        | $=$ boundary state vector, $(\Psi_1, \Psi_2, \dots, \Psi_n)$ |

## Subscript

|     |                                |
|-----|--------------------------------|
| $i$ | $=$ $i$ th component of vector |
|-----|--------------------------------|

## Superscript

|       |                      |
|-------|----------------------|
| $(i)$ | $=$ $i$ th iteration |
|-------|----------------------|

## LITERATURE CITED

1. Chang, K. S., and S. G. Bankoff, *AIChE J.*, **15**, 000 (1969).
2. Bilous, O., and Amundson, N. R., *Chem. Eng. Sci.*, **5**, 81, 115 (1956).

Manuscript received October 26, 1967; revision received April 15, 1968; paper accepted April 22, 1968.